Case study II: Modelling the transmission of a thin film

Adam Stone
Department of Materials Science and Engineering, Lehigh University, Bethlehem, PA 18015, USA
(Dated: July 20, 2011)

A curve fitting analysis based on the Levenberg-Marquardt algorithm was applied to optical power transmission data for thin films of different thicknesses, yielding information about film thickness, refractive index dispersion, and absorption characteristics of the films. Both individual and simultaneous fits were performed for three films of the same material but varying thickness, and the difficulties in fitting a much thicker film of a different material were discussed.

The optical power transmission through an interface at near-normal incidence angle from some material (1) into another material (2), T_{12}, is related to the amplitude transmission coefficient, t_{12}, according to:

$$T_{12} = \frac{n_2}{n_1} t_{12}^2 = \frac{n_2}{n_1} \left(\frac{2n_1}{n_1 + n_2} \right)^2 \tag{1}$$

The amplitude transmission coefficient given in the problem statement (Eq. 2) describes the combined effect of two interfaces in the form of a thin film, with an additional complex term to account for the interference effects that arise in such films with multiple internal reflections.

$$t_f = \frac{t_{af} t_{fs}}{1 - \frac{r_{fa} r_{fs}}{e^{\alpha d}} e^{i2n_f dk}} e^{-\alpha d}, \tag{2}$$

In order to fit the experimental data, the power transmission must be calculated from Eq. 2 according to Eq. 1. Since t_f includes two individual transmission coefficients (an air-to-film term, t_{af}, and a film-to-substrate term, t_{fs}), The power transmission through the film will be given by:

$$T_f = \frac{n_f}{n_a} \frac{n_s}{n_f} |t_f^2| = n_s |t_f^2|, \tag{3}$$

Here the absolute value is necessary due to the imaginary component. Since the light must also pass through the substrate and the substrate-air interface, an additional factor of $(1 - R_{sa})$ must be included to account for its reflection. The power reflection is related to the amplitude reflection coefficient by:

$$R_{12} = r_{12}^2 = \left(\frac{n_1 - n_2}{n_1 + n_2} \right)^2, \tag{4}$$

Direct use of Eq. 2 in fitting algorithms proved difficult, as simply squaring and applying an absolute value function was ineffective at producing an analytical expression free of imaginary terms that could be fit to the data. Instead, it was noted that the absolute value of a complex square is equivalent to multiplying the expression by its complex conjugate. In doing so, after first converting the exponential to sine and cosine terms according to Euler's formula, the imaginary terms could be cancelled. Thus the full equation for power transmission through the film-substrate assembly is given by:

$$T = \frac{n_s \left(e^{-\alpha d} t_{af} t_{fs}\right)^2 (1 - r_{sa}^2)}{\left(1 - \frac{r_{af} r_{fs}}{e^{\alpha d}} cos(2n_f dk)\right)^2 + \left(\frac{r_{af} r_{fs}}{e^{\alpha d}} sin(2n_f dk)\right)^2} \tag{5}$$

The r and t coefficients are simple relationships between refractive indices extracted from Eqs. 1 and 4 , with the refractive index of the film n_f assumed constant for the first fit. The α absorption parameter was assumed to be a simple Gaussian in frequency, as suggested in the problem statement. Using $\lambda = c/\nu$ this was rewritten in terms of wavelength:

$$\alpha = \alpha_o e^{-\Delta\lambda^2 \left(\frac{1}{\lambda} - \frac{1}{\lambda_o}\right)^2} \tag{6}$$

Substituting the expressions for α, t, and r into Eq. 5 gives the full expression which can be fit to the data. The result of a first set of fits with constant n_f is shown in Fig. 1 for the three data sets.

It is clear that substantial and systematic errors remain after the first fit, especially in the features near the

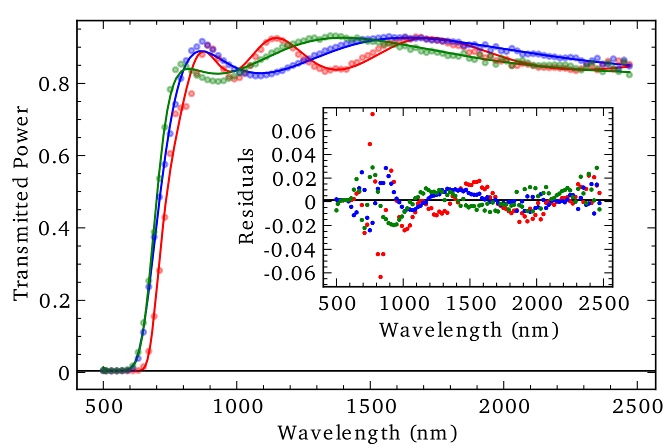

FIG. 1. Best-fit curves and residuals assuming constant n_f.

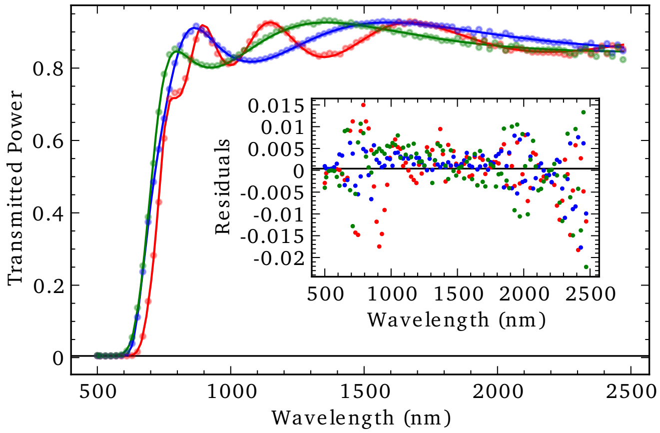

FIG. 2. Best-fit curves and residuals assuming n_f described by Sellmeier equation with single oscillator.

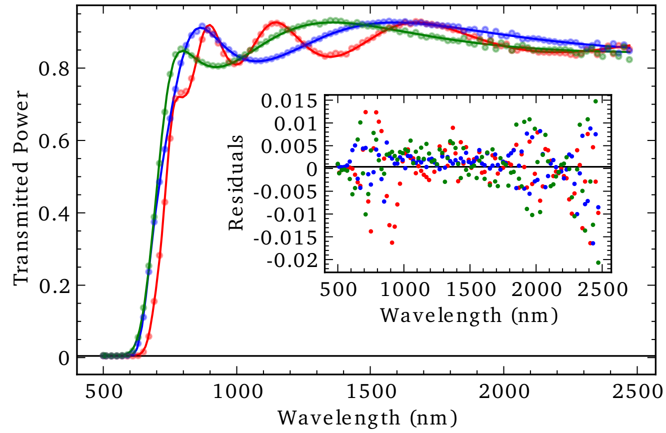

FIG. 3. Best-fit curves and residuals assuming n_f described by Sellmeier equation with single oscillator.

absorption edge. A much better fit can be obtained by accounting for refractive index dispersion in the film with a Sellmeier equation with one oscillator:

$$n_f = \sqrt{1 + \frac{S_1}{1 - (\lambda_1/\lambda)^2}} \tag{7}$$

Fig. 2 shows the fits obtained after making this substitution. The errors near the absorption edge have been greatly reduced, and the residuals look less systematic and more like random noise. However, further improvement may be possible. Adding another oscillator could more accurately describe the refractive index dispersion, but would also require fitting with two more parameters to produce, at best, a very subtle improvement. A slightly smaller χ^2 may not be worth the increased the uncertainty in the best-fit values. Such a two oscillator fit was attempted regardless, but a convergent solution could not attained for any of the three curves, even if the starting guess parameters were tuned to give reasonable agreement with the data before being passed to the fitting algorithm.

A compromise can be found by adding only a single extra parameter to approximate a second oscillator centered at very low wavelengths. The Sellmeier equation in this case would simply include another constant within the square root:

$$n_f = \sqrt{A + \frac{S_1}{1 - (\lambda_1/\lambda)^2}} \tag{8}$$

This approach does produce a convergent fit (Fig. 3), although qualitatively it does not look noticeably different from the single oscillator fit. Quantitatively, the low-λ oscillator approximation does produce an improved χ^2 for all three data sets (Table I). The addition of another parameter in the model does cause the uncertainty in some of the individual fitting parameters to increase, but not to unreasonable levels. It therefore seems that Eq. 8 provides the best model for refractive index dispersion of the films, so the parameters obtained from this model were considered the best-fit results.

TABLE I. Minimized χ^2 values after fits using Eqs. 7 and 8.

	Red Data	Blue Data	Green Data
Eq. 7	3.85×10^{-3}	1.64×10^{-3}	3.60×10^{-3}
Eq. 8	3.01×10^{-3}	1.47×10^{-3}	3.09×10^{-3}

Results

The film thicknesses, refractive index, and absorption parameters obtained from the fits are shown in Table II with errors of one standard deviation (1σ), obtained from the diagonal of the covariance matrix produced by the Levenberg-Marquardt algorithm. As expected, the thickest film corresponds to the data with the most oscil-

TABLE II. Thickness, refractive index, and absorption results for the three films.

	Red Data	Blue Data	Green Data
$d(nm)$	935 ± 2	443 ± 1	375 ± 1
A	1.79 ± 0.04	2.00 ± 0.31	1.92 ± 0.09
$\lambda_1(nm)$	500 ± 0	500 ± 34	499 ± 1
S_1	1.29 ± 0.03	1.11 ± 0.29	1.18 ± 0.07
$\alpha_o(\mu m^{-1})$	5.45 ± 1.29	70.4 ± 46.4	8.62 ± 1.35
$\lambda_o(nm)$	564 ± 11	454 ± 24	545 ± 9
$\Delta\lambda(nm)$	4110 ± 190	2770 ± 220	3710 ± 150

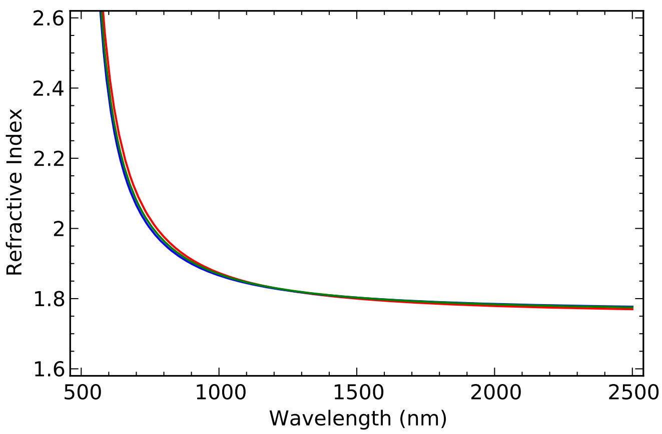

FIG. 4. Refractive index curves obtained from individual fits.

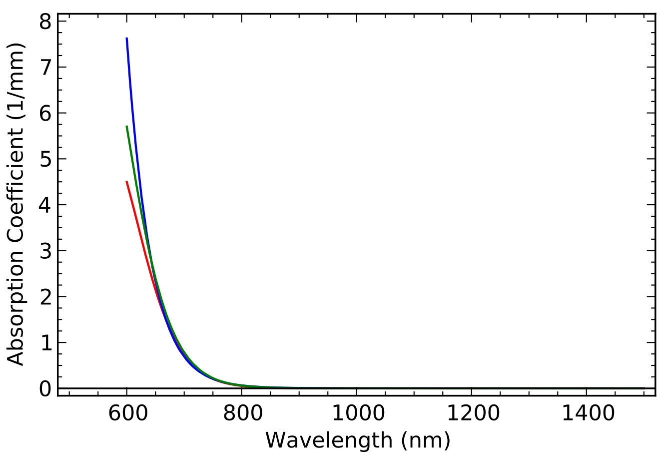

FIG. 5. Absorption edge curves obtained from individual fits.

lations. The refractive index parameters are fairly close between the three films, which one would expect since the films are the same material and their thickness should not affect their inherent refractive index properties. To gauge the significance of these differences in refractive index dispersion suggested by these fits, Eq. 8 is plotted using the obtained parameters in Fig. 4. It should be noted that the largest differences occur before 520 nm, below the absorption edge, and that the curves within the range where the transmission is nonzero are very close.

The absorption parameters vary more substantially between the films even though these should also in principle be material parameters. The discrepancy is likely due to only one side of the absorption function being represented by the experimental data. In other words, the data doesn't provide enough information to unambiguously fit the three parameters of the Gaussian absorption model without strong correlations. Thus, despite the disparate values obtained by the fits for the absorption parameters, the absorption edges plotted in

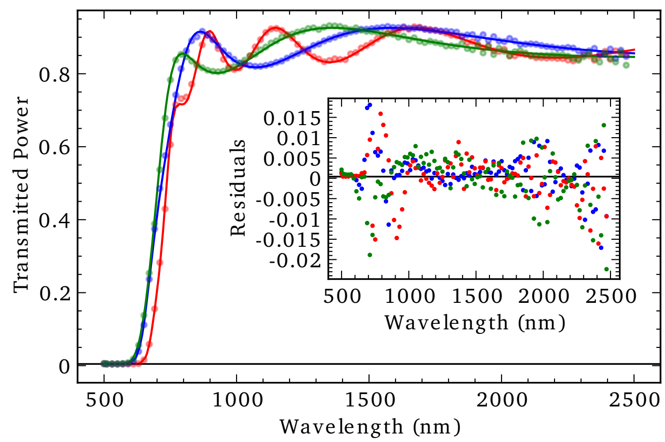

FIG. 6. Best-fit curves and residuals from simultaneous fitting of the three films.

Fig. 5 still look nearly identical.

Simultaneous Fitting

Between the three data sets, the only paramater that should vary in principle is the thickness. The absorption and dispersion characteristics should be material properties. Therefore it would be desirable to fit all three data sets simultaneously rather than individually, such that the common material parameters are optimized for all three data sets. Some curve fitting software may support simultaneous fitting of multiple data sets to a common model, but one can sometimes achieve the same result with typical fitting algorithms as well.

In this case, Eq. 5 becomes approximately constant for wavelength values very far away on either side of the absorption edge. The three data sets can thus be combined into a single data set if they are sufficiently shifted in wavelength with respect to each other. Three copies of Eq. 5, each with a separate d parameter and a wavelength shift equal to the shift applied to the corresponding data set, can then be added together to create a single expression to fit to the combined data.

By ensuring that the data sets are shifted far apart in wavelength, their individual fitting functions within the combined expression will all approach a constant value by the time they overlap the other data sets. The effect is to simply shift the entire curve by some constant value while avoiding any distortion in the regions of interest. This shift can then be dealt with by subtracting a constant dy term from the overall fitting expression and including it as a fitting parameter.

This strategy of simultaneous multiple curve fitting was applied successfully using Eq. 8 as the model for refractive index dispersion. A 200,000 nm wavelength

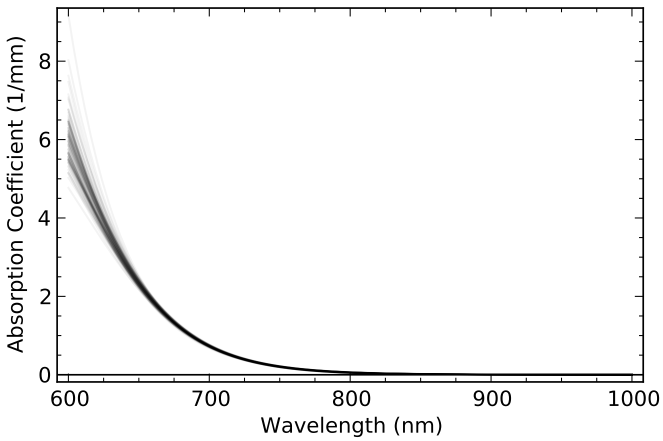

FIG. 7. Absorption edge obtained from simultaneous fitting with Monte Carlo interpolation assuming $\sigma = 0.02$ measurement error.

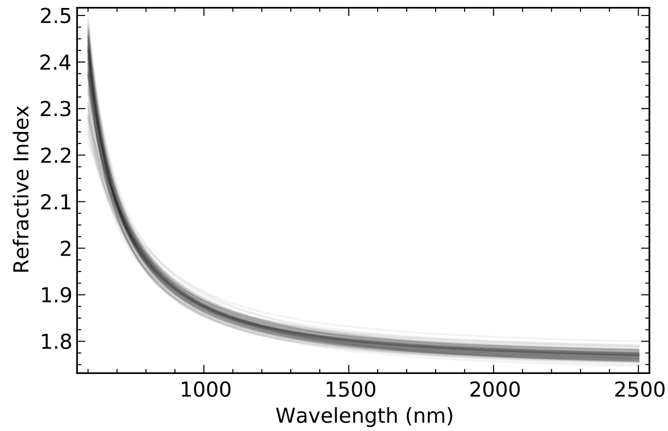

FIG. 8. Refractive index dispersion curve obtained from simultaneous fitting with Monte Carlo interpolation assuming $\sigma = 0.02$ measurement error.

spacing was used between the data sets, and a minimized χ^2 of 0.00941 was obtained. The resulting fit is shown in Fig. 6 (with wavelength shifts removed), and the final parameter values are summarized in Table III.

While the χ^2 of 0.00941 appears to be worse than with the individual fits, this is to be expected since the number of fitting parameters has effectively been decreased by replacing three independent sets of absorption and dispersion parameters (which really shouldn't have been independent from a physical standpoint) with a single set for all three films. This final result therefore probably represents the better fit.

The absorption and refractive index curves can be plotted with the parameters obtained from this multiple-curve fit. In order to get a sense of the precision of these curves, a Monte-Carlo approach can be used in which new artificial data sets are interpolated from the model fit to the original data and then each of these is fit and plotted as well. The results of such an analysis, assuming a gaussian measurement error in transmission with a 0.02 standard deviation, are shown in Figs. 7 and 8. Since the data goes to zero transmission below 600 nm, only the curves above 600 nm are shown.

High Frequency Oscillations

A fourth data set containing oscillations of much higher frequency was also included in the problem statement. The higher frequency oscillations suggest that the film should be much thicker. Initial attempts to refine parameter guess values suggest that the substrate material is also different. The average transmission in this sample is lower than the previous films, so a higher refractive index must be assumed if the substrate material is the

TABLE III. Thickness, refractive index, and absorption results for simultaneous fitting of the three films, $\pm 1\sigma$.

$d_{red}(nm)$	936 ± 2
$d_{blue}(nm)$	441 ± 1
$d_{green}(nm)$	376 ± 1
A	1.81 ± 0.14
$\lambda_1(nm)$	500 ± 14
S_1	1.27 ± 0.14
$\alpha_o(\mu m^{-1})$	11.0 ± 1.7
$\lambda_o(nm)$	531 ± 7
$\Delta\lambda(nm)$	3640 ± 100

same. However, the film's refractive index determines the amplitude of the oscillations; using a high enough index to reduce the average absorption to match the data forces the amplitude of the oscillations to become too large. The substrate's refractive index must therefore be included in the fit.

The large number of oscillations spaced closely together makes fitting this data more difficult. It is much harder to find guess parameters to give the proper peak locations and spacings since so many more peaks must be aligned, and a small misalignment has a large effect on χ^2 because the slope between oscillations is so steep. Refractive index dispersion also has a strong effect on the fit in this case because of its influence on peak spacing.

Many initial guesses were found to produce convergent fits, but with large χ^2 and very poor agreement with the data. This suggests there are many local minima in the parameter space in which the fitting algorithm can become trapped without producing a satisfactory fit, which proved to be the most challenging hurdle to fitting the data: the guess parameters had to be very close to the

TABLE IV. Thickness, refractive index, and absorption results for the thick film and substrate, $\pm 1\sigma$.

$d(nm)$	11598 ± 9
A	4.33 ± 0.02
$\lambda_1(nm)$	448 ± 1
S_1	2.59 ± 0.02
$\lambda_s(nm)$	539 ± 5
S_s	1.57 ± 0.02
$\alpha_o(\mu m^{-1})$	0.68 ± 0.11
$\lambda_o(nm)$	584 ± 5
$\Delta\lambda(nm)$	6190 ± 170

final result before a good fit could be found. This effectively defeated the purpose of using a curve fitting algorithm in the first place, since the answer had to be effectively known in advance, or found by manually adjusting parameters by trial-and-error.

Despite these difficulties, a fairly good fit was eventually found by varying the initial guess for λ_1 by 10 nm increments after finding guess parameters that got somewhat close to the general shape of the data. The refractive index of the film was modeled with Eq. 8, while the substrate was modeled with Eq. 7 (with parameters S_s and λ_s) after it was observed that a constant n_s seemed unable to reproduce the oscillation amplitude over the full length of the data. The final parameter values are summarized in Table IV. The final fit, shown in Fig. 9, had a χ^2 of 0.129. The residuals plot (inset) shows that some systematic error remains, suggesting the fit could be further improved in principle; but given the challenges described above, the effort required would probably not be worth the minor improvement.

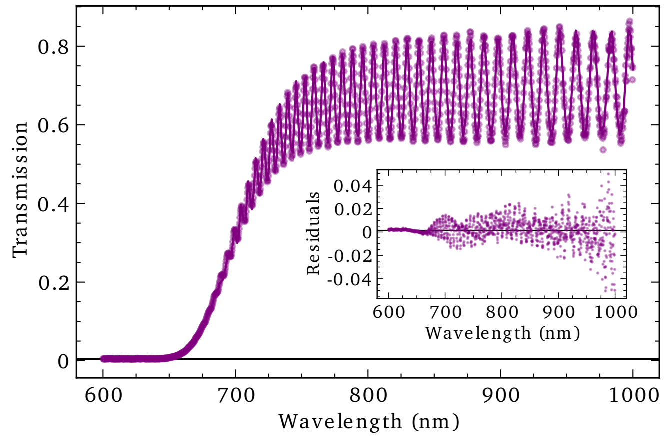

FIG. 9. Best-fit curves and residuals for the thick film.

Conclusion

The Levenberg-Marquardt algorithm is a useful tool for analyzing experimental data and extracting physical parameters along with estimated fitting errors, provided that a physical model equation is known in advance and approximate values for guess parameters can be found. Complicated data with many local χ^2 minima in the parameter space, such as the film with many narrowly spaced oscillations, presents a significant challenge and requires that initial guess values be fairly close to the final result before a good fit can be obtained.